European Journal of Mechanics B/Fluids 48 (2014) 13–18

Contents lists available at ScienceDirect

European Journal of Mechanics B/Fluids

journal homepage: www.elsevier.com/locate/ejmflu

Bottom pressure distribution under a solitonic wave reflecting on a vertical wall

Julien Touboul [a,b,*], Efim Pelinovsky [c,d,e,f]

[a] Université de Toulon, CNRS/INSU, IRD, MIO, UM 110, 83957 La Garde, France
[b] Aix Marseille Université, CNRS/INSU, IRD, MIO, UM 110, 13288 Marseille, France
[c] Institute of Applied Physics, Nizhny Novgorod, Russia
[d] Nizhny Novgorod, State Technical University, Nizhny Novgorod, Russia
[e] National Research University, Higher School of Economics, Russia
[f] Institute for Analysis, Johannes Kepler University, Linz, Austria

HIGHLIGHTS

- Travelling and fully reflected solitonic waves are propagated numerically.
- A first approach solves numerically the fully nonlinear potential equations.
- A second one is based on the solution of the Green–Naghdi system of equations.
- Bottom pressure distributions and runup heights obtained are analysed and compared.
- Green–Naghdi equations predict satisfactorily the evolution of the bottom pressure.

ARTICLE INFO

Article history:
Received 14 November 2013
Received in revised form
20 March 2014
Accepted 22 March 2014
Available online 2 April 2014

Keywords:
Bottom pressure distribution
Dispersion influence
Travelling waves
Reflected waves

ABSTRACT

The bottom pressure distribution under solitonic waves, travelling or fully reflected at a wall is analysed here. Results given by two kind of numerical models are compared. One of the models is based on the Green–Naghdi equations, while the other one is based on the fully nonlinear potential equations. The two models differ through the way in which wave dispersion is taken into account. This approach allows us to emphasize the influence of dispersion, in the case of travelling or fully reflected waves. The Green–Naghdi model is found to predict well the bottom pressure distribution, even when the quantitative representation of the runup height is not satisfactorily described.

1. Introduction

The description of the bottom pressure distribution beneath nonlinear surface waves has several motivations. Among these motivations, bottom pressure sensors have long been used to measure surface waves, mainly in the low-frequency range. In the case of very long waves, like tides and tsunamis, the pressure is hydrostatic, and recovering of surface elevation from the data of bottom sensors is quite straightforward. Wind waves, however, are not long even in the coastal zone, and non-hydrostatic (dispersive) corrections play a significant role. Spectral methods, based on transfer functions, are often used to reconstruct the water elevation taking into account the assumption of linearity of waves [1–8]. Meanwhile, the linear hypothesis does not hold when the amplitude of the waves increases, and as it is shown in [3], the linear prediction for largest waves underestimates the results of about 15%. The pressure under nonlinear progressive periodic and solitary waves is found in [9–11], and a map from pressure to surface is presented in [12–14].

The wave behaviour near the coast (cliffs or vertical barriers) in the process of the wave reflection is more complicated. For instance, the relation between wave elevation and bottom pressure is not straightforward, due to the interaction of the incident and

* Corresponding author at: Université de Toulon, CNRS/INSU, IRD, MIO, UM 110, 83957 La Garde, France.
E-mail addresses: julien.touboul@univ-tln.fr, julien.touboul@irphe.univ-mrs.fr (J. Touboul), pelinovsky@hydro.appl.sci-nnov.ru (E. Pelinovsky).

http://dx.doi.org/10.1016/j.euromechflu.2014.03.011
0997-7546/

reflected waves [15]. Furthermore, the head-on-head collision of solitary waves or the soliton reflection from the wall is not elastic, and a dispersive tail appears behind the soliton [16–22]. If the solitary wave has large amplitude, near the wall the wave amplitude in the resulting field may exceed the limiting value and the instability on the wave crest induces the highest slash on such walls [23]. In such conditions, a thin jet generated on the crest of colliding waves was observed numerically in [24], where a detailed study of the collision of high amplitude solitary waves is provided. This jet on the crest of colliding waves should lead to the significant decreasing of the pressure and therefore in the wave action on the wall, but the pressure in such nonlinear wave field, in our knowledge, has not been studied yet.

The question of modelling bottom pressure distribution under nonlinear water waves is often important in problems involving wave propagation, transformation, and beach runup in fairly large and complex areas. The computational cost inherent to such problems being extremely important, the knowledge of simplified models is essential for simulation purposes. Indeed, since the Indian Ocean tsunami of 2004, it became obvious that nonlinear and dispersive effects could play a major role in such processes. Recent progress in Boussinesq-Type models allowed them to describe these effects better. This is why several of these models (FUNWAVE, COULWAVE, GloBouss) nonlinear and dispersive are often used to model tsunami waves. These tsunamis might be of seismic origin [25], generated by submarine landslides [26], due to volcanic eruptions [27], or even storm induced [28].

Still, the limitations of these methods are known. The classical equations (see, for example, [29]) incorporate only weak dispersion and weak nonlinearity, and in practice their range of applicability is limited to $kh < 0.75$. This shortcoming has attracted considerable attention in the recent past, period during which a number of enhanced and higher-order Boussinesq equations have been formulated to improve both linear and nonlinear properties. Unfortunately, many of these models are numerically unstable when dealing with large waves [30]. Thus, Boussinesq-type models of various levels of nonlinearity and dispersion are studied theoretically, using and validating several theories [31].

The Green–Naghdi model was the first model taking the full nonlinearity into account, in the framework of weak dispersion. This model is of particular concern when studying Boussinesq-type models, due to its specific mathematical properties. Indeed, as it is pointed out by Le Metayer et al. [32], the mathematical founding principles of this system are rather strong. The derivation of the Green–Naghdi model was achieved through a variational formulation of the Euler equations by Miles and Slmon [33]. A mathematical justification of the Green–Naghdi model was performed by Makarenko [34], and Alvarez-Samaniego and Lannes [35]. Camassa et al. [36] proposed a Hamiltonian formulation of the Green–Naghdi model.

From a physical point of view, the Green–Naghdi system of equations was studied in various contexts, and it was shown to predict important features of the flow (excluding wave breaking) accurately over a wide range of parameters (see for instance [37]). This system of equations is also used to describe two-layer flows. In this framework, it is named the Choi–Camassa system.

The main goal of the given paper is to analyse the ability of the Green–Naghdi model to describe bottom pressure variation in the process of the soliton reflection from a vertical wall. This analysis is performed numerically in the framework of fully nonlinear Euler equations (Section 2) and the weakly dispersive fully nonlinear Green–Naghdi system (Section 3). Results of computations for travelling and reflected waves are discussed respectively in Sections 4.1 and 4.2.

2. Numerical solution of the fully nonlinear equations

2.1. Basic equations of the problem

The problem is solved by assuming that the fluid is inviscid, incompressible, and the motion irrotational. Thus, the velocity field is given by $u = \nabla\phi$, where the velocity potential $\phi(x, z, t)$ satisfies Laplace's equation. The domain is bounded by the free surface, a horizontal solid bottom and two vertical solid walls. The horizontal and vertical coordinates are x and z respectively whereas t is the time. The still-water level lies at $z = 0$, and the horizontal impermeable bed is located at $z = -H$. The dynamic free surface condition states that the pressure at the surface, $z = \eta(x, t)$, is nil. Assuming the free surface to be impermeable, the problem to be solved is Laplace's equation with the kinematic and dynamic free surface boundary conditions, and the bottom boundary condition.

$$\begin{cases} \Delta\phi = 0 & \text{in } -h \le z \le \eta(x,t), \\ \dfrac{\partial\eta}{\partial t} + \dfrac{\partial\phi}{\partial x}\dfrac{\partial\eta}{\partial x} = \dfrac{\partial\phi}{\partial z} & \text{on } z = \eta(x,t), \\ \dfrac{\partial\phi}{\partial t} + \dfrac{(\nabla\phi)^2}{2} + g\eta = 0 & \text{on } z = \eta(x,t), \\ \dfrac{\partial\phi}{\partial z} = 0 & \text{on } z = -H \end{cases} \tag{1}$$

g being the acceleration due to gravity and ρ the water density. Once the velocity potential and its gradient are known in the fluid, the bottom pressure is obtained by using Bernoulli's equation

$$\frac{p}{\rho} = gh - \frac{\partial\phi}{\partial t} - \frac{(\nabla\phi)^2}{2} \quad \text{on } z = -H. \tag{2}$$

2.2. Numerical approach

A Boundary Integral Equation Method (BIEM) is used to solve the system of equations (1) with a mixed Euler Lagrange (MEL) time marching scheme. Full details of this numerical approach can be found in [38]. This method was already used to investigate the propagation of solitonic waves in [24].

The method is based on the use of Green's second identity, to solve Laplace's equation for the velocity potential.

$$\int_{\partial\Omega} \Phi(\mathrm{P})\frac{\partial G}{\partial n}(\mathrm{P},\mathrm{Q})d\ell - \int_{\partial\Omega} \frac{\partial\Phi}{\partial n}(\mathrm{P})G(\mathrm{P},\mathrm{Q})d\ell = c(\mathrm{Q})\Phi(\mathrm{Q}), \tag{3}$$

where G is the free space Green's function. The fluid domain boundary $\partial\Omega$ is $\partial\Omega_B \cup \partial\Omega_F$, which correspond respectively to solid boundaries and to the free surface boundary. Since P and Q refer to two points of the fluid domain, and since $c(\mathrm{Q})$ is given by

$$c(\mathrm{Q}) = \begin{cases} 0 & \text{if Q is outside the fluid domain}\Omega \\ \alpha & \text{if Q is on the fluid boundary } \partial\Omega \\ 2\pi & \text{if Q is inside the fluid}\Omega, \end{cases} \tag{4}$$

a discretization of this integral equation can be obtained. Time stepping is performed by means of a fourth order Runge & Kutta scheme, with a constant time step. The bottom pressure is calculated by using a finite-difference method.

2.3. Initial condition

We consider a rectangular wave tank of length L and constant depth h with two vertical solid walls located at its ends. The horizontal length of the domain, L, is assumed to be large enough to avoid any perturbation generated from the vertical walls during the computational time of the simulations. For the results concerning propagative waves, a single solitary wave is considered, initially

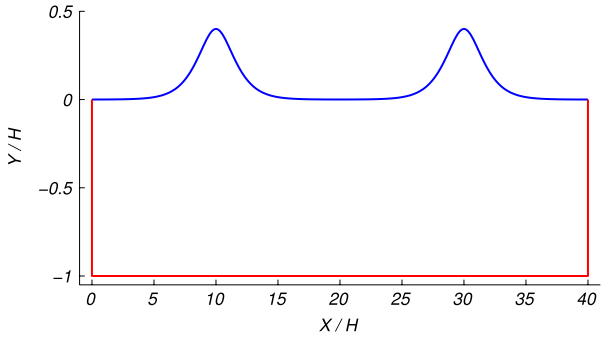

Fig. 1. Initial displacement of the free surface for solitonic waves of initial amplitude $a/h = 0.4$.

located at $X_0/h = 10$. Time evolution of pressure and elevation are provided at $X/h = 20$, which corresponds to the centre of the numerical wave tank. For the results involving reflection at wall, two solitary waves propagating in opposite directions are considered. Indeed, wall reflection is equivalent to the problem of two solitary waves of equal amplitude colliding, but this choice is better suited for numerical considerations inherent to the method of solution. This collision occurs in the middle of the tank ($X/h = 20$). In both cases, the initial free surface is represented by solitary waves computed by using the method initially introduced by Tanaka [39]. The initial free surface elevation, for the case involving two waves of initial $a/h = 0.4$, is shown in Fig. 1. The number of collocation points was considered to be $N_{FS} = 750$ on the free surface, while $N_{BO} = 700$. The nondimensional time step ($\tilde{t} = t\sqrt{g/h}$) varied, from a simulation to the other, from $dt = 10^{-2}$ to $dt = 10^{-4}$. Numerical checks were performed, and errors on mass conservation never exceeded $2 \cdot 10^{-4}$.

3. Numerical solution of the Green–Naghdi equations

3.1. The Green–Naghdi equations

The Green–Naghdi equations were initially introduced by Green and Naghdi [40]. These equations can be obtained by considering a thin layer of an incompressible, inviscid fluid. The shallow water approximation is introduced in Euler equations by assuming that the horizontal velocity field is independent from depth. Thus, it corresponds to an *ab initio* guess of the structure of the vertical velocity component. The vertical integration of the Euler equations leads to the formulation of the Green–Naghdi system, which reads, in its classical form, and for one dimension of propagation,

$$\begin{aligned}&\frac{\partial u}{\partial t} + u\frac{\partial u}{\partial x} + g\frac{\partial \sigma}{\partial x}\\ &\quad = -\frac{1}{\sigma}\frac{\partial}{\partial x}\left[\frac{1}{3}\sigma^3\left(\frac{\partial^2 u}{\partial t\partial x} + u\frac{\partial^2 u}{\partial x^2} - \left(\frac{\partial u}{\partial x}\right)^2\right)\right],\\ &\frac{\partial \sigma}{\partial t} + \frac{\partial(\sigma u)}{\partial x} = 0.\end{aligned} \tag{5}$$

Here, u refers to a layer averaged horizontal velocity component, and σ is the local depth, which corresponds to the surface elevation for problems in constant depth H ($\sigma = \eta + H$). A comprehensive derivation of the Green–Naghdi system can be found in [41]. The system can be equivalently rewritten in a conservative form, leading to the formulation

$$\begin{aligned}&\frac{\mathrm{D}u}{\mathrm{D}t} + g\frac{\partial \sigma}{\partial x} = -\frac{1}{3\sigma}\frac{\partial}{\partial x}\left(\sigma^2\frac{\mathrm{D}^2\sigma}{\mathrm{D}t^2}\right),\\ &\frac{\mathrm{D}\sigma}{\mathrm{D}t} + \sigma\frac{\partial u}{\partial x} = 0.\end{aligned} \tag{6}$$

The symbol $\mathrm{D}/\mathrm{D}t$ should be understood as a material derivative, meaning that $\mathrm{D}/\mathrm{D}t = \partial/\partial t + u\partial/\partial x$.

Once this system of equations is solved, the bottom pressure distribution can be obtained by

$$\frac{p}{\rho} = g\sigma - \frac{\sigma^2}{2}\left(\frac{\partial^2 u}{\partial t\partial x} + u\frac{\partial^2 u}{\partial x^2} - \left(\frac{\partial u}{\partial x}\right)^2\right), \tag{7}$$

as it was pointed out by Pelinovsky and Choi [42] and Pelinovsky [43].

The Green–Naghdi equations are often used in the framework of high amplitude water waves propagating in shallow water, since they provide fully nonlinear solutions of the problem, under the assumption of weak dispersion. In its classical formulation, these equations are especially appreciated since they correspond to a Galilean invariant model, which is conservative for a positive definite energy [32].

3.2. Numerical approach

In this work, we perform a numerical solution of the GN system. The method of solution used corresponds to the numerical scheme introduced by Pearce and Esler [44]. The solution algorithm is pseudo-spectral. The equations system (5) is transformed in a vorticity-divergence form, as detailed in [44]. This allows time-derivatives to appear implicitly in the divergence equation only. Thus, the difficulty reduces to solve a nonlinear equation at each time-step in order to determine the divergence tendency. This equation can be solved by iterating in spectral space to determine each Fourier component. The time stepping is then performed by using standard multi-step schemes (Euler of time step $dt/2$ and centred leap frog of time step dt for the initial time stepping, centred leap frog of time step $2dt$ for the following time steps). However, these authors implemented a hyper-diffusive term to dissipate the turbulent down-scale cascade of enstrophy, but this *ad-hoc* diffusive term turned out to be unnecessary in the framework of our simulations.

3.3. Initial condition

The numerical wave tank considered here is quite similar to the one considered in the previous section. Reference length L and depth h are taken to be equal to those considered with the BIEM approach. The boundary conditions, however, have to be periodic, since the approach used here is pseudo-spectral. However, length L considered is assumed to be large enough to avoid any perturbation generated from these boundaries during the computational time of the simulations. As done in the framework of the BIEM approach, a single solitary wave is considered for the results concerning travelling waves. For examining the reflection, two solitary waves propagating in opposite directions are considered, for the reason evoked previously. The collision occurs in the middle of the tank. Thus, the initial free surface is represented by two solitary waves.

Several expressions can be considered to describe solitonic waves in the framework of the Green–Naghdi system of equations. First, a solution of the Korteweg–de Vries equation, second, the solution of exact potential equations, as obtained by Tanaka [39], and third, the soliton derived by Su and Gardner [45] and Zheleznyak and Pelinovsky [46], and also described in Le Metayer et al. [32], which is solution of the Green–Naghdi system. This solution reads

$$\begin{aligned}&\sigma = \eta + H = H + A\,\mathrm{sech}^2\left(B\left(x - Vt\right)\right) \quad \text{and}\\ &u = V\frac{\eta}{\eta + H}, \quad \text{where}\\ &B = \sqrt{\left(\frac{3A}{4(A+H)}\right)} \quad \text{and} \quad V = \sqrt{gH}\sqrt{1 + \frac{A}{H}}.\end{aligned} \tag{8}$$

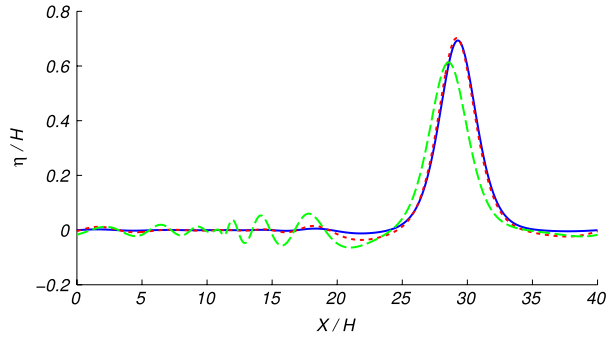

Fig. 2. Free surface elevation obtained by solving numerically the Green–Naghdi system of equations. Solutions are plotted after $N_{ite} = 1500$ time steps, with $dt = 0.01$. $(\cdots)$ is obtained by using KdV soliton as the initial condition, $(- -)$ corresponds to the Tanaka soliton, and $(—)$ is the GN soliton.

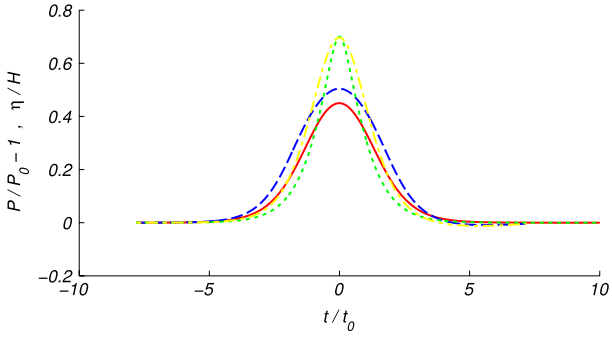

Fig. 3. Time evolution of the normalized water elevation corresponding to a travelling wave of initial $a/H = 0.7$ obtained with full potential equations $(\cdots)$, and with Green–Naghdi equations $(- \cdot -)$. Time evolution of the corresponding normalized bottom pressure obtained with full potential equations $(—)$, and with Green–Naghdi equations $(- -)$.

These initial conditions were propagated with the numerical solver of the Green–Naghdi system of equations, during $N_{ite} = 1500$ time steps. The results obtained are presented in Fig. 2. Given the results, the soliton corresponding to Eq. (8) was used as the initial condition for these simulations, instead of using the Tanaka soliton as it is performed within the BIEM approach.

For each simulation, the number of collocation points was considered to be $N_{FS} = 2^{10}$ on the free surface. The time step used was equal to $dt = 10^{-2}$. The relaxation parameter varied from $\gamma = 0.5$ to $\gamma = 0.2$ from a simulation to another. Numerical checks were performed, and errors on mass conservation never exceeded 10^{-5}.

4. Results and discussion

4.1. Results for travelling waves

Fig. 3 presents the time evolution of the normalized water elevation and bottom pressure deviation from hydrostatic pressure, corresponding to a travelling wave of initial $a/H = 0.7$ obtained with both numerical approaches, which is close to the limiting amplitude $a/H = 0.78$ for stable solitary waves [47]. The normalization of the free surface is made with respect to the water depth at rest H, while the normalization of the bottom pressure is made with respect to the corresponding hydrostatic pressure ($P_0 = \rho g H$). For the sake of readability, this normalized hydrostatic pressure (equal to unity) is subtracted to the plot, so that the bottom pressure term $P/P_0 - 1$ can be understood as the deviation from the state at rest, due to the presence of the soliton. Green and yellow lines correspond to normalized water elevation obtained respectively with fully nonlinear equations and the Green–Naghdi

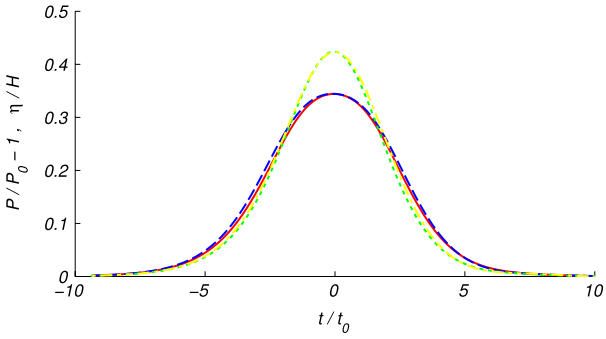

Fig. 4. Time evolution of the normalized water elevation corresponding to a soliton of initial $a/H = 0.2$ reflecting at a wall, obtained with full potential equations $(\cdots)$, and with Green–Naghdi equations $(- \cdot -)$. Time evolution of the corresponding normalized bottom pressure obtained with full potential equations $(—)$, and with Green–Naghdi equations $(- -)$.

system. Red and blue lines are the time evolution of the normalized pressure, minus hydrostatic contribution, obtained respectively with fully nonlinear approach and Green–Naghdi equations.

From this figure, a good qualitative behavior of the Green–Naghdi system is observed. The maximum elevations reached by both methods of solutions are very similar. The associated bottom pressure distribution presents a similar bell-shaped evolution. The maximum values of the bottom pressure distribution reached through both methods, however, differ slightly. The Green–Naghdi approach turns out to overestimate the maximum bottom pressure distribution by 10%. The width of the bell-shaped curves are slightly different, which is understood through the differences among soliton solutions used in both approaches. Indeed the soliton introduced by Le Metayer et al. [32] is wider than Tanaka soliton, as can be seen by comparing both elevations in Fig. 3.

4.2. Results for waves fully reflected

Fig. 4 presents the time evolution of the normalized water elevation and bottom pressure deviation from hydrostatic pressure, corresponding to a weakly nonlinear wave of initial $a/H = 0.2$ reflecting at a vertical wall, obtained with both numerical approaches. Green and yellow lines correspond to normalized water elevation obtained respectively with fully nonlinear equations and the Green–Naghdi system. Red and blue lines are the time evolution of the normalized pressure, minus hydrostatic contribution, obtained respectively with fully nonlinear approach and Green–Naghdi equations.

The time evolution of the elevation is bell-shaped, as it was for travelling waves. The same behaviour is observed for the bottom pressure distribution, with both models. This result is obtained with weak nonlinearity, and as a matter of fact, weak dispersion.

On the other hand, Fig. 5 presents the time evolution of the normalized water elevation and bottom pressure deviation from hydrostatic pressure, corresponding to a wave of initial $a/H = 0.7$ reflecting at a vertical wall, obtained with both numerical approaches. Here again, green and red lines are obtained with fully nonlinear equations, while yellow and blue correspond to the Green–Naghdi system.

Here, the time evolution of the elevation is bell-shaped, as it was for travelling waves. But, concerning the pressure evolution, it is highly interesting to notice the difference with the previous case. Here, the bottom pressure distribution presents a local minimum at a moment close to the maximum runup. It could be explained by the formation of a residual freely falling jet, which has been previously observed by Chambarel et al. [24]. This phenomenon was confirmed here. Surprisingly it is also reproduced by the GN model

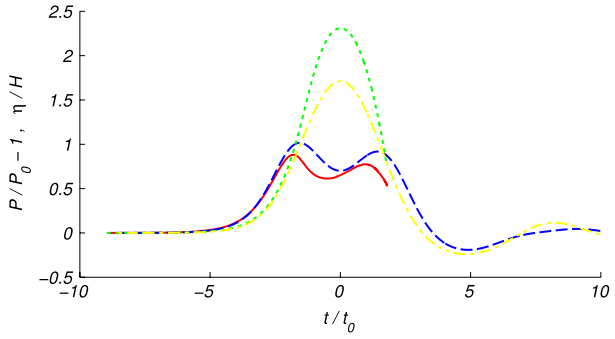

Fig. 5. Time evolution of the normalized water elevation corresponding to a soliton of initial $a/H = 0.7$ reflecting at a wall, obtained with full potential equations $(\cdots)$, and with Green–Naghdi equations $(- \cdot -)$. Time evolution of the corresponding normalized bottom pressure obtained with full potential equations $(-)$ and with Green–Naghdi equations $(- -)$.

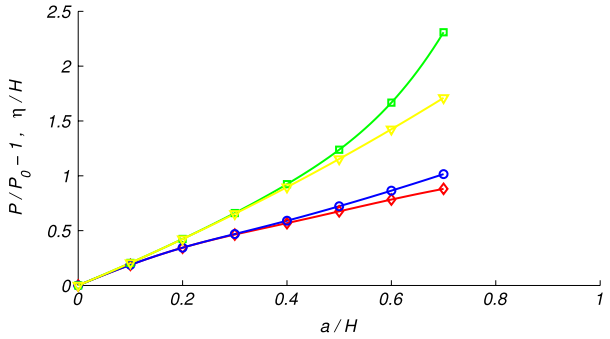

Fig. 6. Maximum normalized elevation and bottom pressure reached during the run-up process as a function of nonlinear parameter a/H. (□): maximum elevation within fully nonlinear equations, (∇): maximum elevation within Green–Naghdi equations, (◇): maximum bottom pressure within fully equations model, and (○): maximum bottom pressure within Green–Naghdi equations.

where the vertical motion of water particles is not resolved explicitly. Thus, long wave models of Boussinesq-like type can explain this physical phenomenon for very steep nonlinear waves. When considering the moment for which this minimum is observed, a slight difference between both models is observed. Indeed, the local minimum described by the Green–Naghdi system is observed when the maximum runup is reached, while it is observed earlier than the maximum runup height in the framework of the fully nonlinear equations. An explanation to this observation might be found in the integrable nature of both systems. The Green–Naghdi model is a near-integrable model of water waves. A fully integrable system would have provided an elastic reflection of the soliton at the wall, and both evolution curves (elevation and pressure) would have been symmetric around the collision time. The weak non-integrability of the Green–Naghdi system is responsible for a small asymmetry, which is observed in the curves. The second local maximum of the pressure is slightly smaller than the first local maximum, which is due to the radiation of soliton energy into the dispersive tail. Fully potential theory is non-integrable, and such asymmetric effects (inequality of peaks, and time shift with respect to the maximum runup time) are more visible.

For the quantitative agreement, however, both Green–Naghdi and fully nonlinear models present discrepancies. The Green–Naghdi system of equations underestimates the runup height by 25%, while the maximum bottom pressure is underestimated by the Green–Naghdi system by 12%.

The quantitative evolution of these quantities, namely the maximum runup height and the maximum bottom pressure, as a function of the nonlinear parameter a/H are presented in Fig. 6. Green and yellow lines correspond to normalized maximum runup obtained respectively with fully nonlinear equations and the Green–Naghdi system. Red and blue lines are maximum values reached by the normalized pressure during the runup phase, obtained respectively with fully nonlinear approach and Green–Naghdi equations.

From this figure, it appears that the Green–Naghdi equations provide a good agreement, even for fully reflected waves, in the range of nonlinear parameter $a/H = 0 - 0.5$. For larger values of this parameter, this system of equations underestimates runup heights, while it overestimates maximum pressure values. Indeed, for $a/H > 0.5$, the discrepancies between the two models are less significant when comparing the maximum pressure than when comparing the maximum runup heights.

4.3. Discussion

Given the results for both travelling and fully reflected waves, it appears that the Green–Naghdi system of equations provides a good qualitative agreement for describing the behaviour of the bottom pressure distribution under solitonic waves. In both cases, the bell-shaped behaviour, present or not, is well described through the Green–Naghdi equations. The simplification of this system based on the hypothesis of weak dispersion, and classically used, is not amenable to keep this property.

When looking at the quantitative agreement, the agreement between both approaches is very good in the framework of travelling waves, while this agreement becomes worse when considering fully reflected waves. This last remark emphasizes that the reflection of waves, which is often observed in coastal areas where pressure transducers are used to recover free surface elevation, should definitively be taken into account in the inverse models.

Acknowledgements

EP thanks partial supports from RFBR Grant (14-05-00092), Austrian Science Foundation (FWF) under project P 246710, VolkswagenStiftung, and highly appreciates the offered opportunity to work as a Visiting Researcher at Université de Toulon. JT acknowledges support from Direction Générale de l'Armement (DGA) and Agence Nationale de la Recherche (ANR) through the Grant ANR-13-ASTR-0007.

References

[1] L. Cavaleri, Wave measurement using pressure transducer, Oceanologia Acta 3 (3) (1980) 339–345.
[2] H. Wang, D.Y. Lee, A. Garcia, Time series surface-wave recovery from pressure gage, Coastal Eng. 10 (4) (1986) 379–393.
[3] C.T. Bishop, M.A. Donelan, Measuring waves with pressure transducers, Coastal Eng. 11 (4) (1987) 309–328.
[4] Y.Y. Kuo, Y.F. Chiu, Transfer function between the wave height and wave pressure for progressive waves, Coastal Eng. 23 (1–2) (1994) 81–93.
[5] A. Baquerizo, M. Losada, Transfer function between wave height and wave pressure for progressive waves, Coastal Eng. 24 (1995) 351–353.
[6] M.M. Zaslavsky, V.P. Krasitsky, About recovery of surface wave spectrum from pressure sensor, Oceanology 41 (2) (2001) 195–200.
[7] C.H. Tsai, M.C. Huang, F.J. Young, Y.C. Lin, H.W. Li, On the recovery of surface wave by pressure transfer function, Ocean Eng. 32 (10) (2005) 1247–1259.
[8] M.C. Huang, C.H. Tsai, Pressure transfer function in time and time-frequency domains, Ocean Eng. 35 (2008) 1203–1210.
[9] J. Escher, T. Schlurmann, On the recovery of the free surface from the pressure within periodic travelling water waves, J. Nonlinear Math. Phys. 15 (2) (2008) 50–57.
[10] A. Constantin, W. Strauss, Pressure beneath a Stokes wave, Comm. Pure Appl. Math. 63 (2010) 533–557.
[11] A. Constantin, J. Escher, H.C. Hsu, Pressure beneath a solitary water wave: mathematical theory and experiments, Arch. Ration. Mech. Anal. 201 (2011) 251–269.
[12] A. Constantin, On the recovery of solitary wave profiles from pressure measurements, J. Fluid Mech. 699 (2012) 376–384.
[13] K.L. Oliveras, V. Vasan, B. Deconinck, D. Henderson, Recovering the water wave profile from pressure measurement, SIAM J. Appl. Math 72 (3) (2012) 897–918.

[14] D. Clamond, A. Constantin, Recovery of steady periodic wave profiles from pressure measurements at the bed, J. Fluid Mech. 714 (2013) 463–475.
[15] J. Touboul, V. Rey, Bottom pressure distribution due to wave scattering near a submerged obstacle, J. Fluid Mech. 702 (2012) 444–459.
[16] T. Maxworthy, Experiments on collisions between solitary waves, J. Fluid Mech. 76 (1976) 177–185.
[17] C.H. Su, R.M. Mirie, Collisions between two solitary waves, J. Fluid Mech. 98 (1980) 509–525.
[18] R.M. Mirie, C.H. Su, Collisions between two solitary waves. Partt 2: a numerical study, J. Fluid Mech. 115 (1982) 475–492.
[19] J. Byatt-Smith, On the change of amplitude of interacting solitary waves, J. Fluid Mech. 182 (1987) 485–497.
[20] J. Byatt-Smith, The reflection of a solitary wave by a vertical wall, J. Fluid Mech. 197 (1988) 503–521.
[21] M.J. Cooker, P.D. Weidman, D.S. Bale, Reflection of a high-amplitude solitary wave at a vertical wall, J. Fluid Mech. 342 (1997) 141–158.
[22] W. Craig, P. Guyenne, J. Hammack, D. Henderson, S. C, Solitary water wave interactions, Phys. Fluids 18 (1997) 057106.
[23] M.S. Longuet-Higgins, D. Drazen, On steep gravity waves meeting a vertical wall: a triple instability, J. Fluid Mech. 466 (2002) 305–318.
[24] J. Chambarel, C. Kharif, J. Touboul, Head-on collision of two solitary waves and residual falling jet formation, Nonlinear Processes Geophys. 16 (2009) 111–122.
[25] F. Lovholt, G. Kaiser, S. Glimsdal, L. Scheele, C.B. Harbitz, G. Pedersen, Modeling propagation and inundation of the 11 March 2011 Tohoku tsunami, Nat. Hazards Earth Sys. Sci. 12 (4) (2012) 1017–1028.
[26] P. Watts, S.T. Grilli, J.T. Kirby, G.J. Fryer, D.R. Tappin, Landslide tsunami case studies using a Boussinesq model and a fully nonlinear tsunami generation model, Nat. Hazard Earth Sys. Sci. 3 (2003) 391–402.
[27] T. Torsvik, R. Paris, I. Didenkulova, E. Pelinovsky, A. Belousov, M. Belousova, Numerical simulation of a tsunami event during the 1996 volcanic eruption in Karymskoye lake, Kamchatka, Russia, Nat. Hazards Earth Syst. Sci. 10 (2010) 2359–2369.
[28] K.F. Cheung, A.C. Phadke, Y. Wei, R. Rojas, Y.J.M. Douyere, C.D. Martino, P.L.F. Liu, P.J. Lynett, N. Dodd, S. Liao, E. Nakazaki, Modeling of storm-induced coastal flooding for emergency management, Ocean. Eng. 30 (2003) 1353–1386.
[29] D.H. Peregrine, Long waves on a beach, J. Fluid Mech. 27 (04) (1967) 815–827.
[30] F. Lovholt, G. Pedersen, Modeling propagation and inundation of the 11 March 2011 Tohoku tsunami, Internat. J. Numer. Methods Fluids 61 (6) (2009) 607–637.
[31] P.A. Madsen, H.B. Bingham, H.A. Schaffer, Boussinesq-type formulations for fully nonlinear and extremely dispersive water waves: derivation and analysis, Proc. R. Soc. Lond. A. 459 (2003) 1075–1104.
[32] O. Le Metayer, S. Gavrilyuk, S. Hank, A numerical scheme for the Green–Naghdi model, J. Comput. Phys. 229 (2010) 2034–2045.
[33] J. Miles, R. Salmon, Weakly dispersive nonlinear gravity waves, J. Fluid Mech. 157 (1985) 519–531.
[34] N. Makarenko, A second long-wave approximation in the Cauchy–Poisson problem, Dyn. Contin. Media 77 (1986) 56–72.
[35] B. Alvarez-Samaniego, D. Lannes, Large time existence for 3D water waves and asymptotics, Invent. Math. 171 (2008) 485–541.
[36] R. Camassa, D.D. Holm, C.D. Levermore, Long-time effects of bottom topography in shallow water, Physica D 98 (1996) 258–286.
[37] B.T. Nadiga, L.G. Margolin, P.K. Smolarkiewicz, Different approximations of shallow water fluid flow over an obstacle, Phys. Fluids 8 (1996) 2066–2077.
[38] J. Touboul, C. Kharif, Two-dimensional direct numerical simulations of the dynamics of rogue waves under wind action, in: Q. Ma (Ed.), Advances In Numerical Simulation of Nonlinear Water Waves, in: Advances in Coastal and Ocean Eng., vol. 11, World Scientific, 2010, pp. 43–74.
[39] M. Tanaka, The stability of solitary waves, Phys. Fluids 29 (1986) 650–655.
[40] A.E. Green, P.M. Naghdi, A derivation of equations for wave propagation in water of variable depth, J. Fluid Mech. 78 (1976) 237–246.
[41] C.H. Borzi, R.A. Kraenkel, M.A. Manna, A. Pereira, Nonlinear dynamics of short travelling capilary-gravity waves, Phys. Rev. E 71 (2005) 026307.
[42] E. Pelinovsky, H.S. Choi, A Mathematical model for nonlinear waves due to moving disturbances in a basin of variable depth, J. Korean Soc. Coastal Ocean Engineers 5 (3) (1993) 191–197.
[43] E. Pelinovsky, Hydrodynamics of Tsunami Waves, Applied Physics Institute Press, Nizhny Novgorod, 1996.
[44] J.D. Pearce, J.G. Esler, A pseudo-spectral algorithm and test cases for the numerical simulation of the two-dimensional rotating Green–Naghdi shallow water equations, J. Comput. Phys. 229 (2010) 7594–7608.
[45] C.H. Su, C.S. Gardner, Korteweg–de Vries equation and generalizations. III. Derivation of the Korteweg–de Vries equation and Burgers equation, J. Math. Phys. 10 (1969) 536–539.
[46] M.I. Zheleznyak, E.N. Pelinovsky, Physical and mathematical models of the tsunami climbing a beach, in: E.N. Pelinovsky (Ed.), Tsunami Climbing a Beach, Applied Physics Institute Press, Gorky, 1985, pp. 8–34.
[47] M.S. Longuet-Higgins, M. Tanaka, On the crest instabilities of steep surface waves, J. Fluid Mech. 336 (1997) 51–68.